Proceedings World Geothermal Congress 2023
Beijing, China, April 17 – 21, 2023

Characterization and Geothermal Potential of the Kenya Rift Floor outside the Central Volcanoes: Case Study of the Otutu Rift, Kenya Central Rift

Erique Nyawir, Peter O. Omenda and Jacques Varet

KenGen PLC, P.O. Box 785-20117, Naivasha, Kenya

ENyawir@kengen.co.ke

Keywords: Geothermal, Geochemistry, Geology, Otutu, Kenya Rift, Badlands, Eburru, Elmenteita

ABSTRACT

Otutu rift is part of the larger Kenya Central Rift and lies in between the Eburru and Elmenteita volcanic field, within the larger Kenya Rift Valley. The area covers a longer portion of the rift floor thus becomes a good representative of the active rift segment. Geological and geochemical surface exploration studies were undertaken in the area, an area outside the normal central volcanoes so as to understand the areas' geothermal relevance. This allowed for more data and information acquisition on the areas' volcanology and more so the surface mineralogical and chemical characteristics of the volcanic lavas within the study area. This study gives us a better understanding of the behavior of a rift segment. During fieldwork, several geological structures were mapped and several samples collected for further analysis. A wide variety of lava rocks were identified and these included alkali olivine basalts, trachytes and abundant. The petrochemical results from both ICP-MS and ICP-AES included the rock composition in terms of major oxides, trace and rare earth elements. These results were used to plot various diagrams that included the variation diagrams (for both major oxides and trace elements), Total Alkali-Silica diagram, the AFM diagram, CIPW Norm Classification and also normalized Rare Earth Elements plots. These results provided a complete view of the various kind of liquids emitted during the last million years along this active segment of the rift. It can, therefore, be concluded that the Otutu rift is an important heat release area. It possibly have a shallow underlying anomalous mantle along the rift axis, where successive magma rejuvenations have taken place. This is supported by the steam vents that are aligned along open fissures and faults synchronous and post-dating the volcanic events. These results are of interest for the future geothermal development of the area. However, further studies are recommended on the area including geochronological studies, a close-knit geophysical surveys (to clearly map out the heat sources) and a detailed mineralogical study of a few key phases determining the major shifts in the fractionation process.

1. INTRODUCTION

Otutu rift is part of a rift segment that is located on the floor of the KRV between the Eburru and Lake Elmenteita areas. It is approximately 140 km northwest of Nairobi, 11 km northwest of Lake Naivasha. KRV is made of a succession of central volcanoes alternating with single rift segments. Otutu is one of the rift spreading segments (characterized by fissure eruptions) located between the two central volcanoes of Eburru and Menengai (Figure 1).

The floor of the central KRV is characterized by two geologic settings: central volcanoes and flat-lying fissural volcanic fields. The central volcanoes have massifs of the order of 10 to 20 km wide with average reliefs of 100 to 500m above the rift floor. These central volcanoes are averagely-spaced 50 to 70 km from each other and alternate with flat-lying fissural volcanic fields occupying the low lands. The fissural fields are dominated by basaltic and intermediate lavas and interlayered by pyroclastic fall deposits that came from the surrounding central volcanoes and lacustrine sediments that originated from periods of high rift lake levels.

There are several grabens in the Kenya rift formed as a result of rifting. These fault troughs include the Elmenteita volcanic area, the area around Solai and Lake Nakuru. These areas are characterized by widespread fissures and crustal instability. These were formed during the Lower Pleistocene or Lower-Middle Pleistocene epoch, McCall (1957). McCall (1957) notes that the graben in Elmenteita experiences numerous volcanic activities as it is one of the least unstable troughs in the rift. The noted line of instability, where thermal conditions are also noted, appears as the current axis of the rift spreading. This line extends southwards towards Eburru shoulders and further south passing through the western shores of Lake Naivasha towards Ol'Njorowa Gorge within the Hell's Gate National Park.

By looking at the bigger picture of the central segment of the KRV, it is observed that there is a succession of basaltic rift segments (B) that alternate with silicic central volcanoes (C). This can be seen by the following studied areas: Suswa is made of trachytic and phonolitic lavas (C), and thereafter we have the Akira plains with basaltic lavas (B); Olkaria and Longonot-Trachyte and rhyolites (C), then we have the Ndabibi-basalts (B), northwards occur Eburru trachytes and rhyolites (C), then Elmenteita Basaltic lavas (B); then Menengai – trachytes (C), (Clarke et al., 1990).

In terms of geothermal development, it is only in Eburru, Menengai, Olkaria and recently Paka and Korosi geothermal fields where deep drilling activities have taken place until now. Currently, appraisal and exploratory drilling is on-going at Paka and Korosi respectively. These two fields are far north of the earlier-mentioned three geothermal fields with more than 15 deep wells have been drilled so far between them. More than Geographically, the study area is bound between 0°27'S to 0°38'S and 36°11' to 36°21'.

The Kenya Electricity Generating Company, PLC (KenGen) together with Geothermal Development Company (GDC) have been exploring the KRV for its geothermal energy resources in the country so as to provide environmentally clean and low-cost energy for the country. KenGen is currently producing electricity from geothermal resources at Olkaria and Eburru while GDC has undertaken production drilling in Menengai and is currently carrying out exploratory drilling further north, in Paka volcano and Korosi areas.

Additionally, the Government of Kenya has licensed several other geothermal areas to private investors to explore and develop the resources for power generation and direct use.

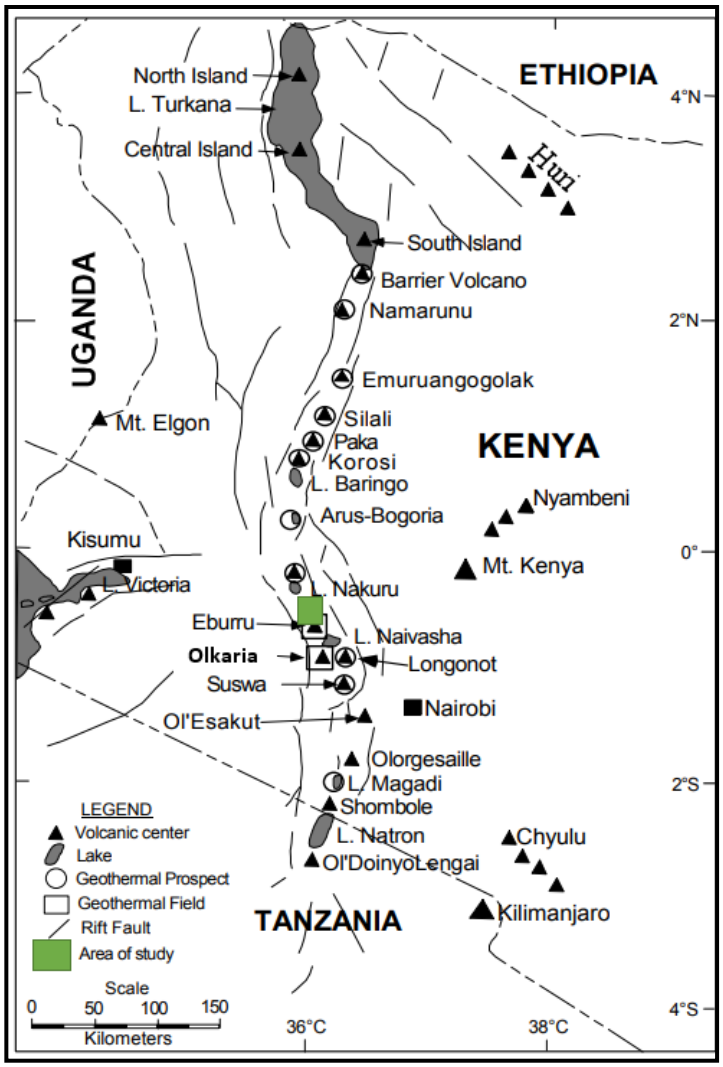

Figure 1: Map of the Kenya Rift showing the location of the Quaternary volcanoes (in black triangles) along the rift axis and the study area (in the green rectangle). Open circles are geothermal prospects in Kenya (Lagat, 2004).

2. RESULTS

2.1 GEOLOGY

Otutu rift was affected by rhythmic phases of spreading, during which dramatic volcano-tectonic events occurred, including both extensional tectonics and magmatic eruptions along the same active N-S trending faults and fissures of the rift axis. These volcanic activities in the rift axis are clearly linked with successive tectonic events characterizing the rift opening. During the fieldwork, it was noted that the whole volcanic activity in the study area is essentially characterized by lava flows, scoria cones and domes, without marked pyroclastic eruptions. The exception was noted in the areas influenced by the shallow water, thus producing hyaloclastites, which are generally easily altered and therefore difficult and unreliable to use for chemical analysis.

Quite a wide variety of differentiated products were observed in the study area, which is essentially a fissural area. It was also observed that shield structures tended to form, built on initial basaltic flows and intermediate terms (hawaiites, mugearites and trachyte flows). But these were cut by successive spreading events (normal faulting), allowing for a new magmatic cycle to occur (including basalts and highly differentiated products like rhyolites). It is worth noting that each of these eruption phases produced a variety of magma types that ranged from basaltic (basalts, basaltic trachy-andesites and trachy-andesites) lavas to trachytes and peralkaline rhyolites. The trachytes mainly occur on the slopes of the Eburru volcano both as shield building lavas and Late-phase flows, and this explains the close affinity with the Eburru Late-phase rhyolites with which they are associated in space. The basaltic lavas which occur at the foot of the Eburru volcano have been found not to co-genetic with the rhyolites and trachytes, which occur at the study area, along the same volcano-tectonic axis known as the Otutu rift. Whereas the evolution of the Eburru lavas was made possible by the thick overburden that allowed for the magma to differentiate at low pressures to form the trachytes and rhyolites, the Elmenteita lava evolved from small size magma chambers at mid-crustal depths. The results further demonstrate that even though the basaltic lavas occur in the same area, they were produced from different mantle sources. Below (from Plates 1 to 8) are some of the images taken of the study area and its surroundings.

Generally, normal faulting is in the same direction, N-S, and is well expressed in this study area with slight variations towards E-W. The exception is in areas that are covered by the most recent – sub-historic – Aa basaltic lava flow in Badlands. In the north-eastern part of the area, they tend to be visibly younger from east to west (that is, towards the rift axis) where they also affect more recent lava flows. The recent "Aa" basaltic flow (Plate 1) characterising the Badlands appears to extend mainly in a transverse, E-W direction. The SW limit of the flow is rectilinear and strikingly trending E-W. Due to its low viscosity, the basaltic flow flowed laterally towards the west, forming deep caves.

Numerous cones are also observed, which correspond to former emission centres. Two variety of cones are clearly distinguished: hyaloclastite rings of large diameter, which pre-date the last sub-aerial basaltic lava flows, and scoria cones contemporaneous with this latest volcanic event, showing the emissive source of these Aa basalt flows. The largest and the most probably spectacular faulted hyaloclastite ring, is Losiriwe or the Sleeping Warrior. This spectacular structure is well seen from the Naivasha-Nakuru road crossing the active rift south of Lake Elmenteita (Plate 2). It has a regular circular shape, with a basal diameter of 1.4 km and a maximum height of 120 m along part of the rim of this 900 m wide cone. This ratio of 1/10 between height and diameter is typical for such subaqueous hyaloclastite rings. As observed above, it is affected by normal faults on both sides and a small graben resulting from an open fissure along its axis, showing that this cone was at some stage in time the spreading axis of the rift. At present, the active axis of the rift is shifted 3 km east, at the level of the two other coalescent hyaloclastite cones elongated along the N-S trending rift axis with a sub-aerial eruptive phase having produced both scoria cone (Plate 3) and a lava lake of basaltic composition.

Further south, these normal faults appear quite spectacular with important throws. Some of them clearly show that the tectonics affected the axis of an elongated shield volcano trending in the same meridian direction. Towards the active rift axis, normal faulting also affects very recent volcanic centres, such as a doubled rimmed scoria cone or an obsidian dome further south (Plate 4). On the western side of the rift axis, normal faulting is less visible, but open faults are still frequent, and attentive observations show that the tectonics was also quite violent there. Several hyaloclastite and scoria cones are cut by the N-S normal faults, which dip west, and some are left with only the western rim, with the central and eastern side having been down faulted and are covered by more recent lava flows emitted along the rift axis as seen in Plate 5.

Plate 1: The researcher standing at the boundary of the Elmenteita volcanic basaltic flow, which is in the background, appearing as a highly vegetative field. In the far background are some of the structures that are aligned along the N-S Rift Axis

Plate 1: One of the distinct structures, Sleeping Warrior, a highly faulted dome that is located between the Elmenteita volcanic area and Lake Elmenteita

Plate 3: View of the most recent scoria cone in the southern part of the Badlands

Plate 4: One of the Recent obsidian domes along the active rift axis cut by open fractures

Plate 5: Cedar Hill, a recent rhyolitic dome made of anorthoclase porphyritic obsidian located to the SE of the Badlands area on the northern slope of Eburru volcano (photo by Varet, 2017)

2.2 PETROGRAPHY

All the collected, over 120, rock samples were subjected to initial petrographic analysis in the field before taking samples to the laboratory for more analysis. Petrographic analysis was used to study the mineralogical evolution, confirm the rock type(s), the alteration minerals, and any other additional minerals not observed by the binocular microscope or the hand lens. Petrographic analysis assisted in;

i. Identification of the rock-forming minerals
ii. Characterization of the rock porosity
iii. Modal analysis (mineralogical composition)
iv. Analysis of the rock sample texture
v. Identifying the mineral phases and sequencing (phenocrysts were used as representatives of magmatic reservoir while groundmass used to depict the mode of eruption)

Rock types present in the study area range from alkali basalts to trachytes and peralkaline rhyolites. Both rhyolites and alkali basalts were found in areas around the Eburru volcano and also in the volcanic field south of Lake Elmenteita. The collected samples were analyzed petrographically, and thereafter, 21 samples were picked based on their location, physical state and rock type for whole-rock analyses.

For petrographic microscope analysis, thin sections were prepared at KenGen's Geology lapidary laboratory in Olkaria, Kenya. The process included sawing of the rock samples, polishing, preparation and characterization in order to determine the samples' mineralogy. The thin sections were thereafter mounted on a petrographic microscope for analysis. For this project, thin sections were analysed in both KenGen' s Geology Laboratory in Kenya and the BRGM laboratory in France using Optika B-353POL and the LEICA DM 4500P Microscope, respectively.

2.3 PETROCHEMISTRY

Twenty-one (21) samples from the over 120 rock samples collected were subjected to whole-rock analysis (analysed for Major, Trace and Rare Earth Elements) using ICP-AES and ICP-MS in UBO, Brest, France. The samples were picked based on the surface outcrops and structures observed, in view of establishing a representative picture of the magmatic variations within Otutu rift (across and along the rift segment in particular). Therefore, aphyric or sub-aphyric samples were selected, as they directly allow to trace the evolution of the liquids. Of course, attention was also paid to the phenocrysts and their composition in the same magma types. It is noted that porphyritic samples were discarded during the critical selection of samples for petrochemical analysis as this study centred on the evolution of the liquid composition. This choice also explains some of the gaps observed in this sequence i.e. trachytes and rhyolites. Whole-rock analysis involved both major and trace/rare elements analysis. Major and trace elements are widely used to test petrogenetic models (Reynolds et al., 1992; Bach et al., 1994; Perfit et al., 1994, 1996, 2001; Wendt et al., 1999; Sims et al., 2002).

2.3.1 Major Oxides

Lower Elmenteita basalts have SiO_2 ranging from 48.26 to 55.46%. However, typical basalts would be in the range of 45 to 52%. This wide range of silica content can be attributed to fractional melting. The MgO and CaO values also range from 3.7 to 6.5% and 6.3 to 11.0%, respectively. These high MgO and CaO are typical major oxide trends of basalts. Upper Elmenteita Basalts have SiO_2 ranging from 48.32 to 55.4%. They also have MgO and CaO values ranging from 3.8 to 6.0% and 6.5 to 10.4%, respectively. Generally, basalts are rich in MgO and Cao but low in silica.

The trachytes consist of Pliocene Gilgil Trachytes and Eburru shield-building trachytes. The early trachyte has 68.21% silica, 0.15% MgO, 0.56% CaO. This is relatively higher than what is noted in the shield building trachytes. The shield-building trachyte has SiO_2 ranging from 63.28 to 67.37% with MgO and CaO being 0.01 to 0.17% and 0.61 to 1.38%, respectively.

The rocks occur on the Eburru volcano, and are dominantly on the northern slopes. The lavas have high SiO_2 contents of 69.2-71.4%. The Fe_2O_3 (t) content are high as they range from 7.33 to 10.1%. The rocks have very low MgO contents of 0.01-0.14%. Their Na_2O and K_2O content ranges between 5.1-7.7% and 4.2-5.0%, respectively. The rhyolites at Eburru have been classified as pantellerites due to their low alumina content as compared to the alkalis (combination of K_2O and Na_2O). In this case, the alumina ranges between 7.11 and 8.8% while the alkali ranges from 9.40 to 11.16%.

(a) Total Alkali-Silica classification

From Figure 2, the TAS Diagram shows a regular trend for all samples, slightly above the alkaline / sub-alkaline dividing line (dotted red on the diagram below), which is typical for all transitional series found elsewhere in the EARV, including Afar (Barberi et al., 1975). The rock sampled ranged from mafic through intermediate to silicic rocks (basalts, trachy-basalts, basaltic trachy-andesites, trachy-andesites, trachytes and rhyolites).

Lower Elmenteita basalts vary in composition from basalt through trachy-basalt to basaltic trachy-andesite. Their alkali content varies from 3.69 to 7.51%, while their silica content varies from 48.31 to 55.46%. All the upper Elmenteita basalts samples except sample EN/EBLE 25A fall under the basalt category. Their normalized silica content varies from 48-49%, with the alkalis part ranging from 4.09-4.49%. Sample EN/EBLE 25A has a relatively high silica content (55.1%) and relatively high alkalis (7.66%).

Generally, the Upper Elmenteita basalts are low in both silica and alkali compared to the Lower Elmenteita basalts. They have a general composition of 45-52% SiO_2 and 2 to 5% alkalis. This is noted in the upper Elmenteita suite but apparently the lower Elmenteita suite seems to be higher in their silica and alkali content. This varying composition noted in these basaltic suite (lower Elmenteita) could be as a result of fractional melting.

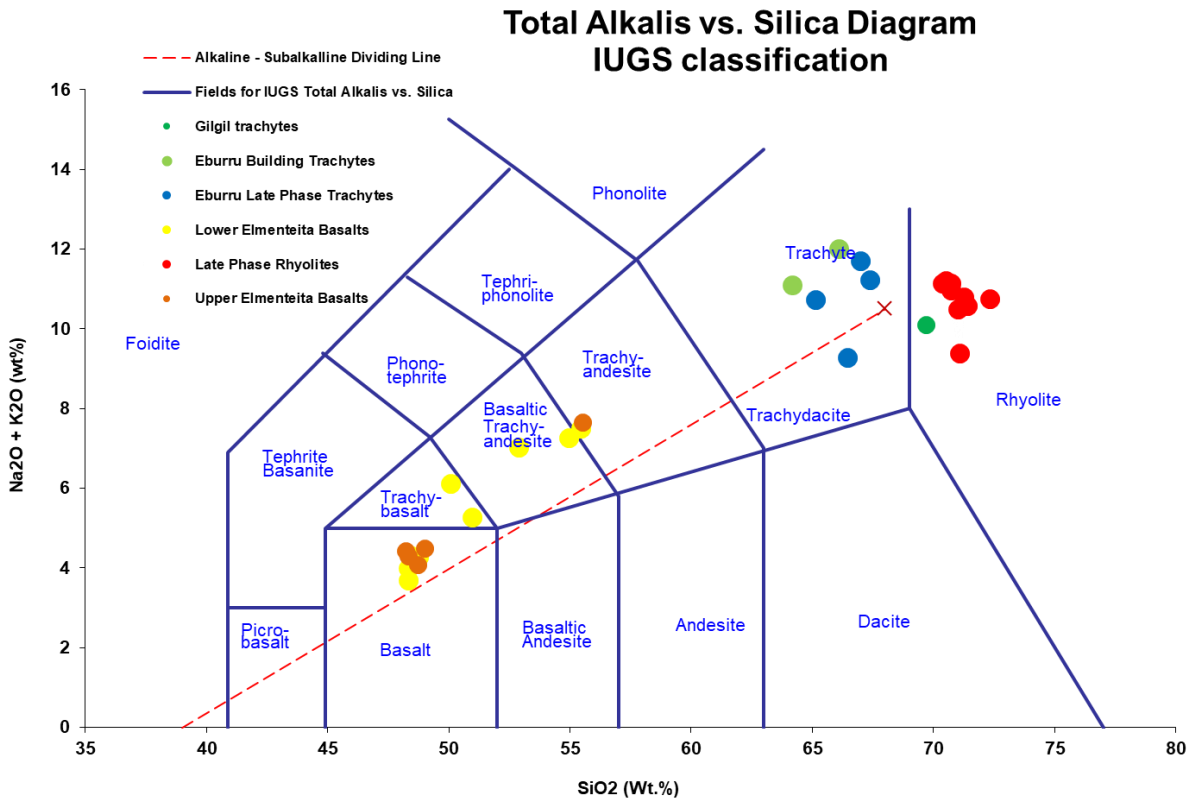

Figure 2: Total Alkali vs Silica Diagram for the study area

The one sample of Gilgil trachyte has high SiO_2 (69.67%), which make it fall within the rhyolite field. However, the petrographic analysis clearly indicates that the lava is trachyte. The lava has an alkali content of 10.12%. Eburru shield trachytes all fell under the trachytes. They had alkali concentrations of 9.3-11.2%, with silica content ranging from 64.2 to 67.4%.

Generally, trachytes are feldspar-rich and thus have 60-65% silica content and an average of 7% alkali. Most of the samples had high silica and alkalic content and were plotted towards the tail end of the trachyte portion in the TAS diagram.

Rhyolite plot with an alkali content of 9.4 to 11.2% while the silica content was 70.4-71.4%. This is expected of rhyolites as they are the most silica-rich igneous rocks. They usually have higher SiO_2 (69-77%) and alkali (>7%).

All the trachyte and rhyolite suites are all silica saturated with concentrations ranging between 64.18 and 71.4% by weight. The suites also have relatively high alkali contents that range between 9.3 to 11.2% and 9.4 to 11.2% by weight, respectively.

Therefore, all the samples plotted above the line that separates the alkaline and sub-alkaline rocks (Figure 2). This means all the rocks are alkaline rocks. Alkaline magmas are known to be derived from mantle-derived basaltic melts. These melts usually have had a residence in the crust and thereafter evolve through the assimilation and fractional crystallization (AFC) processes.

(b) AFM classification

AFM Diagrams, in their classification, distinguishes between the two usual types of parental magmas; alkali and tholeiitic (Figure 3). It is noted that the lavas evolved through depletion of Fe and Mg and enrichment of alkalis. All the samples were plotted below the Tholeiitic (sub-alkaline) series. It is noted that tholeiitic magmas usually form at relatively shallow depths compared to alkalic magmas and differentiate into the SiO_2 oversaturated rhyolites.

Figure 3 shows both trachytic and rhyolitic lavas plotting on the zero MgO axis due to their very low MgO contents while having high contents of alkali and Fe. The evolution of the Elmenteita and Eburru lavas can be described by the fractional crystallization process involving crystallization of ferromagnesian minerals (olivine and pyroxenes) as shown by decreasing Mg and Fe with an evolution from basalt through trachyte to rhyolite. The evolution is characterized by the enrichment of alkalis in the liquid phase.

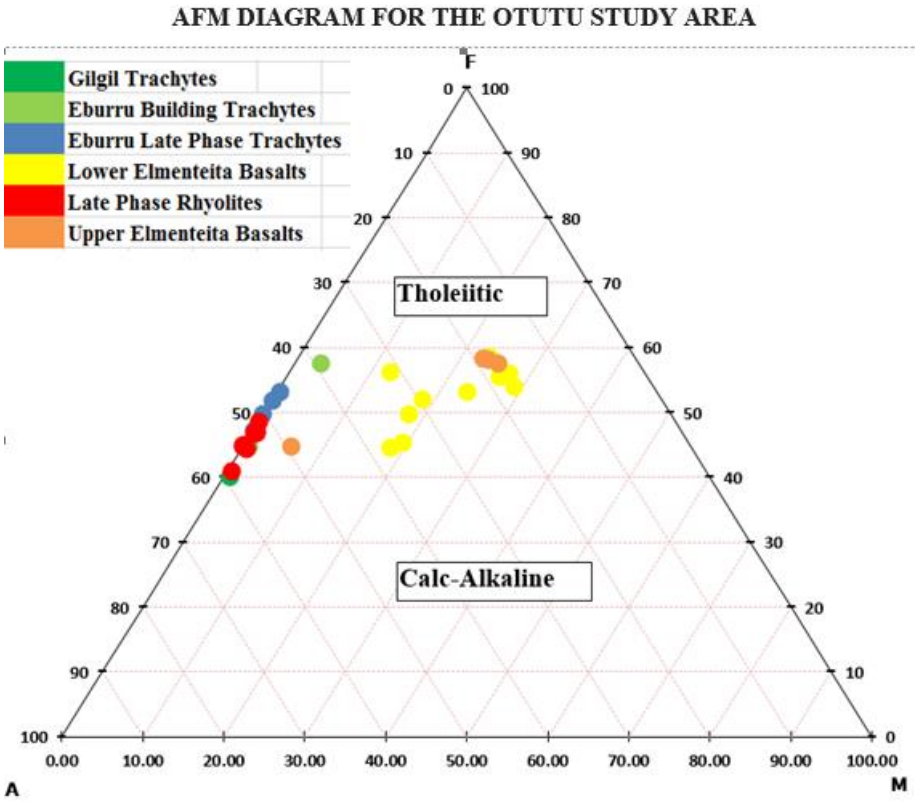

Figure 3: AFM Diagram for the Otutu study area

(c) Harker variation diagrams

Harker variation diagrams were plotted for the various rock suites in the study area. Whereas Upper Elmenteita basalts are younger than the Lower Elmenteita Basalts, they have the highest TiO_2 contents. The graph of SiO_2 vs TiO_2 shows decreasing TiO_2 content from basaltic lava through intermediate lavas to rhyolite (Figure 4). The trend suggests the fractionation of magnetite and/or ilmenite during the evolution of the lavas from basalt to rhyolite. The trend further suggests that the Upper Elmenteita basalts could not be cogenetic with the stratigraphically Lower Elmenteita basalts since they are less evolved.

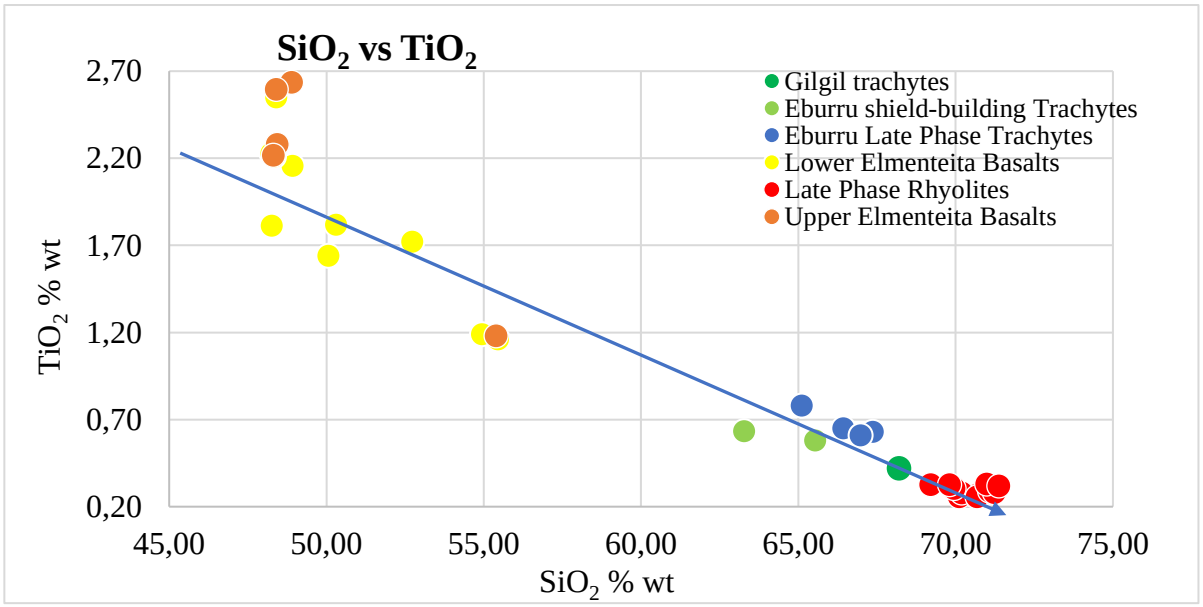

Figure 2.3: SiO_2 vs TiO_2 variation diagram

The Plot of SiO2 vs MgO shows that the basalts at Elmenteita are moderately evolved with SiO2 of 48-55% and MgO contents of between 3.7% and 6.5% (Figure 5). The Lower Elmenteita basalts have some samples with the highest MgO content but show a wide range indicating that the various lava flows are products of different degrees of differentiation. The upper Elmenteita basalts also

have SiO2 of 48-55% but with MgO contents of 3.8 to 6.0%. The wide spread within the Upper basalts indicates that the lava field comprises of a suite of rocks that experienced varying degrees of fractional crystallization. The trachytes and rhyolites have very low MgO suggesting that they are products of protracted fractional crystallization from basaltic liquids.

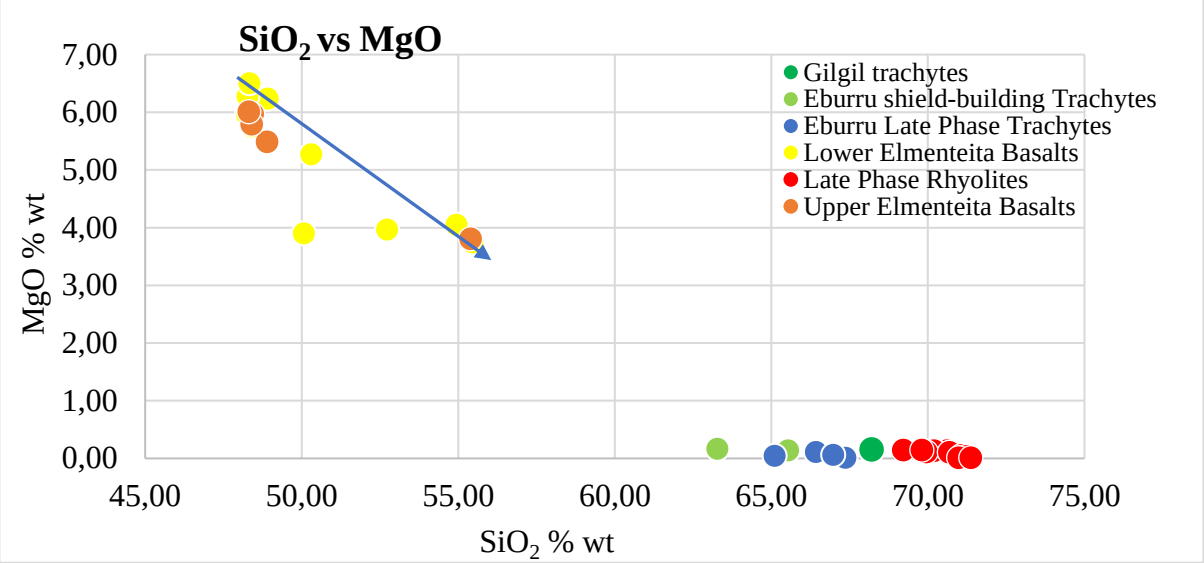

Figure 1: SiO_2 vs MgO variation diagram

Alumina (Al2O3) plot of the study area shows the highest values within the Lower Elmenteita basalts followed by the Upper Elmenteita basalts. However, there is quite a scatter in the plot of the basalts attributed to the incorporation of feldspar crystals in the analysed bulk samples (Figure 6). The plot shows a decreasing trend of Al2O3 with increasing SiO2 with the lowest values in rhyolites and this indicates the role of feldspar fractionation in the evolution of trachytes and rhyolites.

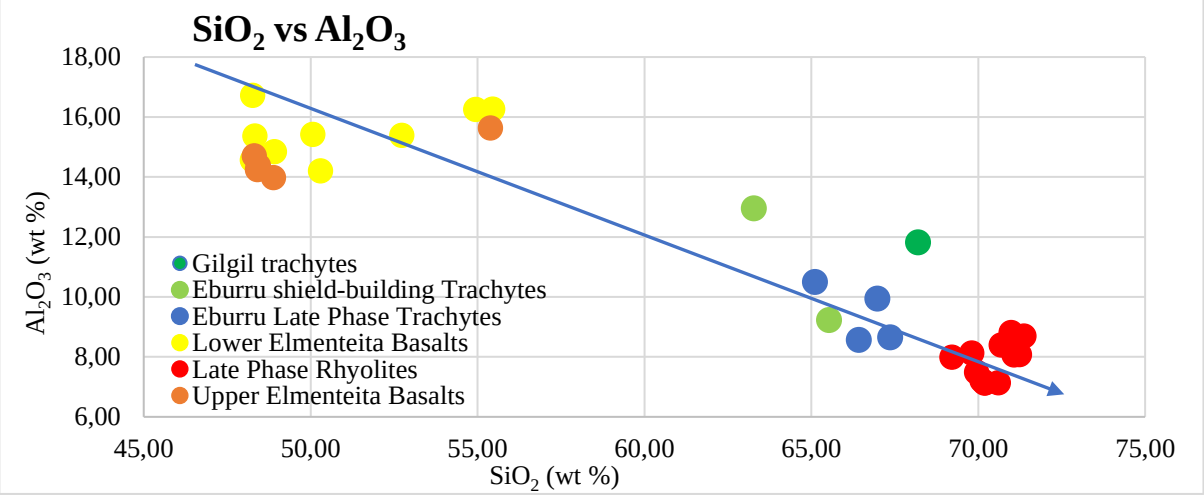

Figure 2: SiO_2 vs Al_2O_3 variation diagram

Variation of total Fe2O3 with SiO2 shows decreasing contents with increasing silica (Figure 7). However, the basalts show a scatter without any clear trends amongst the suite. Rhyolites have the lowest contents, and the data is inconclusive as the basalts seem to fall in a different part of the graph when compared with the trachyte and rhyolites. However, the plot can be interpreted to indicate that trachytes and rhyolites can be generated from basalts by fractionation of Fe-oxide minerals.

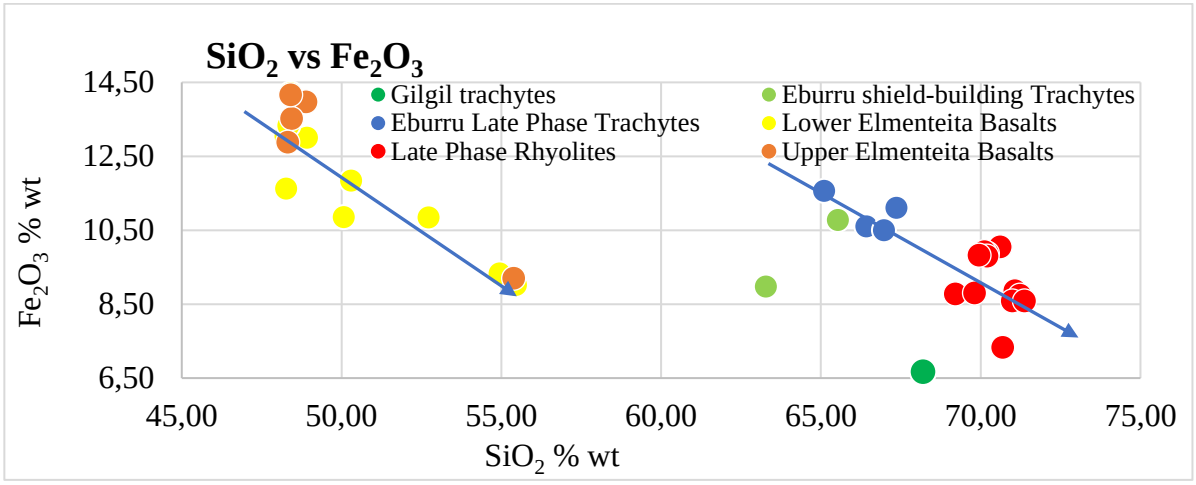

Figure 3: SiO_2 vs Fe_2O_3 variation diagram

SiO2 vs CaO shows a clear reducing trend from basalts through trachyte to rhyolite (Figure 4.8). The graph shows a linear trend within the Lower Elmenteita suite, further confirming that the group has several flows that may be related through the fractional crystallization process. It can be postulated that the cause of the observed trend is the fractionation of calc-plagioclases. Extreme fractional crystallization from trachyte to rhyolites with calc-plagioclases, among other minerals, resulted in the very low values of CaO in the rhyolites.

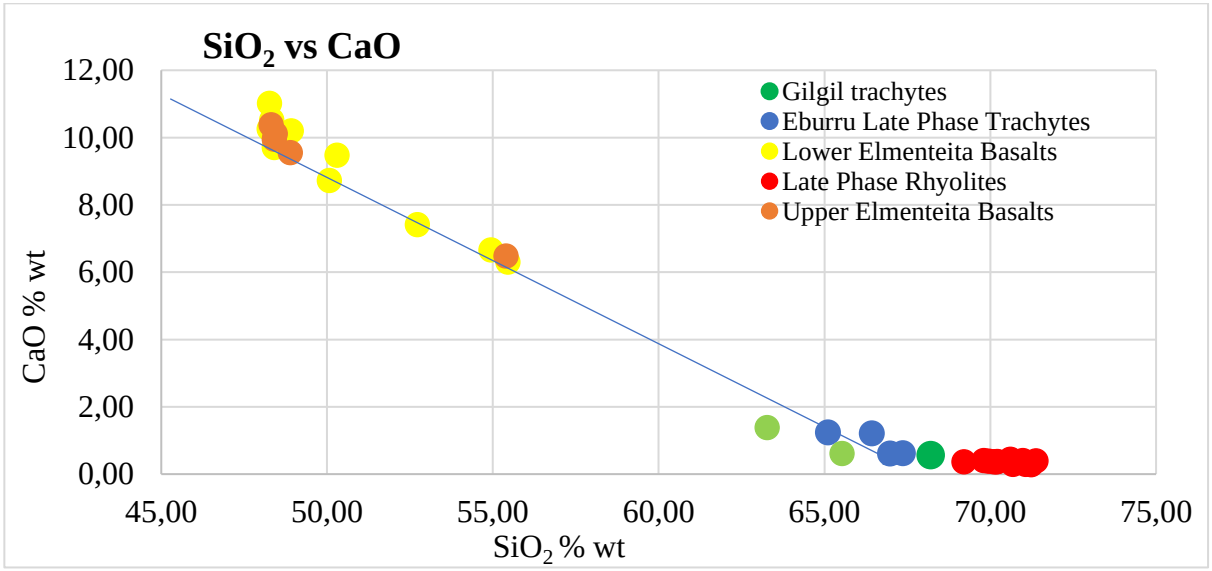

Figure 4: SiO_2 vs CaO variation diagram

P2O5 variation with SiO2 shows the highest values among the Upper and Lower Elmenteita basalts (Figure 9). P2O5 shows a wide linear variation with the Lower Elmenteita basalts suggesting that the lavas that form the formation are related amongst themselves via fractional crystallization. The phosphorus decrease is due to the crystallisation of apatite. Trachytes and rhyolites are very low P2O5 contents which therefore are not in trend with the basalts.

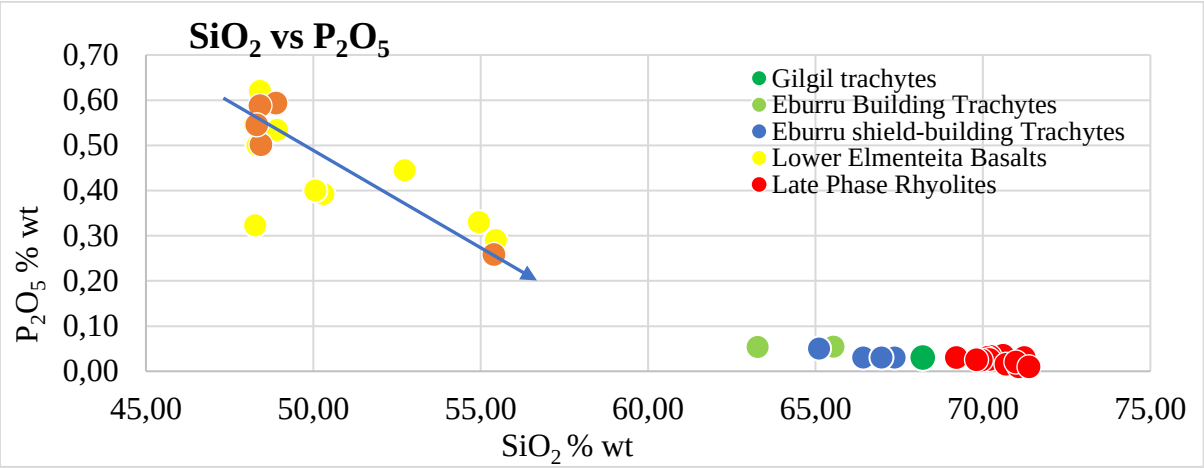

Figure 5: SiO_2 vs P_2O_5 variation diagram

Na_2O and K_2O behave incompatibly during fractional crystallization of liquids from basalts to trachytes and rhyolites, and therefore, their contents increase with SiO_2 (Figures 10 and 11). The strongest incompatibility is recognized from basalts to trachytes, where linear trends are observable. This trend can be attributed to the highly incompatible nature of Na_2O, which results in its enrichment. However, flattening of the curves is noted between trachyte and rhyolite, which can be attributed to the fractionation of feldspars.

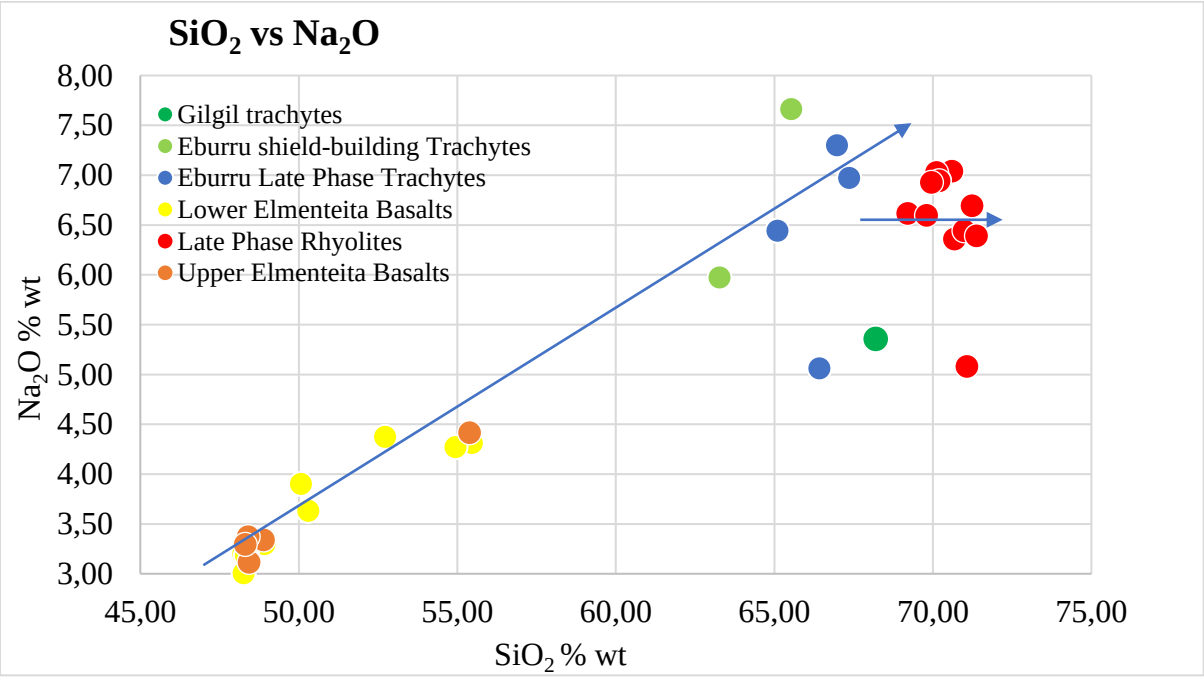

Figure 6: SiO_2 vs Na_2O variation diagram

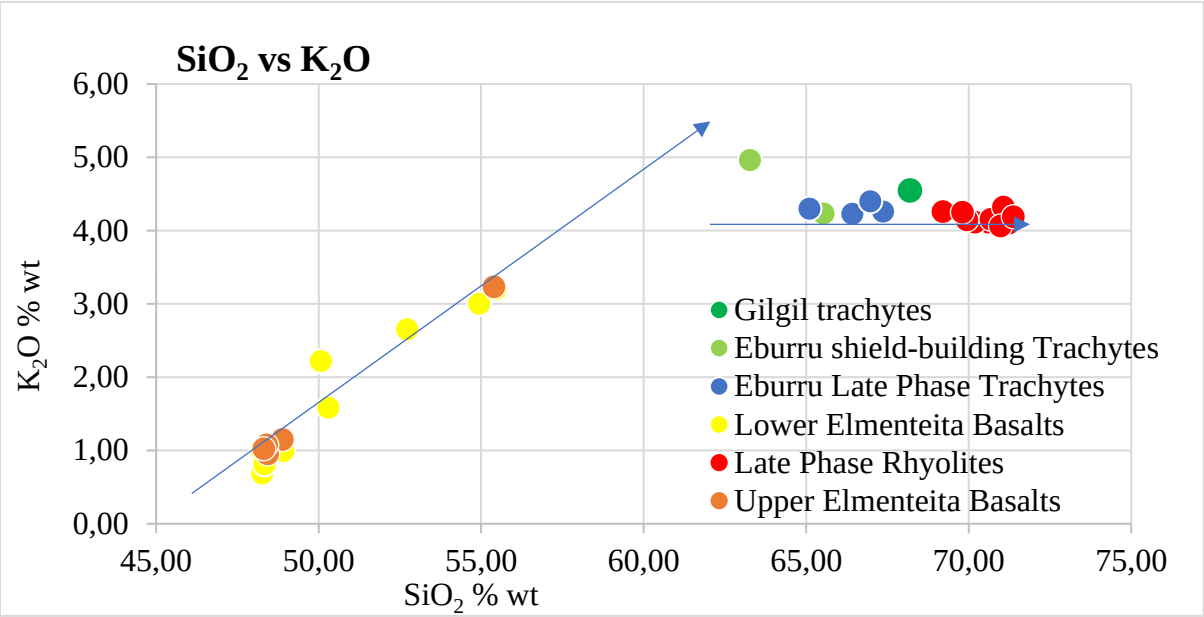

Figure 7: SiO_2 vs K_2O variation diagram

(d) CIPW Norm Classification

The basaltic (lower and upper Elmenteita) samples contain no normative quartz but very high values of normative plagioclase and average normative orthoclase. This ranged between 52.4-62.1% and 5.2-22.3%, respectively. The normative diopside ranged from 10-19.5%, while the normative olivine values ranged from 4.5 to 12.2%. Normative ilmenite varied from 1.3 to 3.2%, and normative magnetite varied from 1.1-18%.

Normative nepheline values were generally low. Values ranging from 0.0 to 3.0% and 0.5 to 1.4% for normative nepheline and apatite, respectively, were also noted, with most samples containing no normative sodium silicate. Normative leucite was absent from all the basaltic samples, which is expected of all sub-alkaline bulk chemistry. The normative zircon ranged from 0.01 to 0.02%, while the normative chromite values were at 0.01%. All the other remaining normative minerals were absent or very low. These included acmite and calcite.

In the trachytic samples, normative quartz was noted. This ranged from 7.8% in sample 13 to 15.9-26.2% in the other samples. The samples also had relatively high values of normative plagioclase and normative orthoclase. This ranged between 22.3-42.3% and 27.7-32.6%, respectively. The normative diopside ranged from 1.8 to 4.6%, while the normative hypersthene values ranged from 5.8 to 10%. Normative acmite varied from 2.3 to 3.9%, while normative sodium silicate varied from 1.8 to 9.8%. Normative ilmenite was low and varied from 0.34-0.9%, while normative magnetite was very low (0.06%) and mostly absent. Normative apatite and zircon values were generally very low. Values ranging from 0.1 to 0.14 % and 0.0 to 0.1 % for normative apatite and zircon were noted, respectively. All the other remaining normative minerals were absent or very low. These included accessory minerals like nepheline, olivine, chromite and calcite.

In the rhyolitic samples, higher normative quartz was noted in comparison to the trachytic samples. This ranged between 30.0-33.1%. The samples also had relatively high values of normative plagioclase and normative orthoclase. This ranged between 14.5-24% and 26.0-28.2%, respectively. This lower plagioclase content in the rhyolites here (as compared to basalts and trachytes) is due to the low alumina deficit. The plagioclase effect usually plays a major role in the generation of peralkaline. The normative diopside was averagely low, ranging from 0.9 to 1.3%, though sample ES1 had 2.7% while the normative hypersthene values ranged from 7.1 to 9.7%. Normative acmite varied from 2.5 to 3.4%, while normative sodium silicate was averagely high, varying from 5.8 to 11.1%. Normative ilmenite was averagely low and varied from 0.3-0.4%, while normative magnetite was very low (0.06%) and mostly absent. Normative apatite and zircon values were generally higher compared to basalts and trachytic suites. Values ranging from 0.02 to 0.08% and 0.18 to 0.24 % for normative apatite and zircon were noted, respectively. All the other remaining normative minerals were absent or very low. These included accessory minerals like nepheline, magnetite, olivine, chromite and calcite.

Generally, by CIPW classification, silicic rocks usually have normative quartz varying from the lower end trachytes through ignimbrites to the higher end rhyolites. The average quartz values are 1-4%, 17-21% and 22-30% for trachytes, ignimbrites and rhyolites, respectively. Silicic rocks also have averagely high values of plagioclase and orthoclase. For silicic rock as a whole, these ranges between 31-55% and 25-30%, respectively.

Most of the basalts show a good balance, with both olivine and hypersthene present, but not quartz (no tholeiite), whereas only 3 samples show the presence of nepheline, mostly as traces (ranging from 0.3-0.4%) with only one sample exceeding 1%, which confirm the transitional character of the basaltic magma source. Whereas olivine is always visible in thin sections under the microscope, orthopyroxene is not observed, which is classical in a basaltic environment (orthopyroxenes rather appear in plutonic environments). However, during the differentiation process, the magma progressively acquires a slight, then dominant, silica saturation in the end products.

Amphiboles are not present in the normative analysis for the simple reason that the CIPW norm is based on "dry" mineral only – pyroxene in this case - and do not allow for amphibole (or mica) to occur. These frequently show signs of instability (mineral internally altered and rimmed with iron oxides) with the groundmass, indicating that these silica-deficient minerals formed at depth are not in equilibrium with the silica-saturated liquid containing them when emitted at the surface in more oxidizing and eventually "dryer" conditions.

2.3.2 Trace Elements

The trace elements results obtained were plotted in variation diagrams while the multi elements (Rare Earth Elements) were normalized (chondrite normalized REE) and thereafter plotted for the study area to show the evolution chemistry,

(a) Variation plots

Process identification plots (PIPs) were plotted to check on how the elements related to each other. PIPs are diagrams plotted of the ratio of two (2) incompatible elements against the abundance of the other. Incompatible elements are part of the trace elements. Figures 12 to 20 show how these elements relate to each other.

La vs La/Ta shows Elmenteita basalts of the lower series having a ratio of 14-18 while the upper Elmenteita basalts have ratio of a 16-19 (Figure 12). The trachytes have a ratio of about 13.5, while the rhyolites have a ratio of about 13. In this plot, Ta is more incompatible than La and therefore is enriched in the liquid phase relative to La. The plot further suggests that the Late-phase Eburru trachyte and Eburru Late-phase rhyolites may be related by fractional crystallization processes. However, the Lower and Upper Elmenteita basalts are different within the suite, as seen by the wide range of rations. The basalts are also not related to the trachyte and rhyolite.

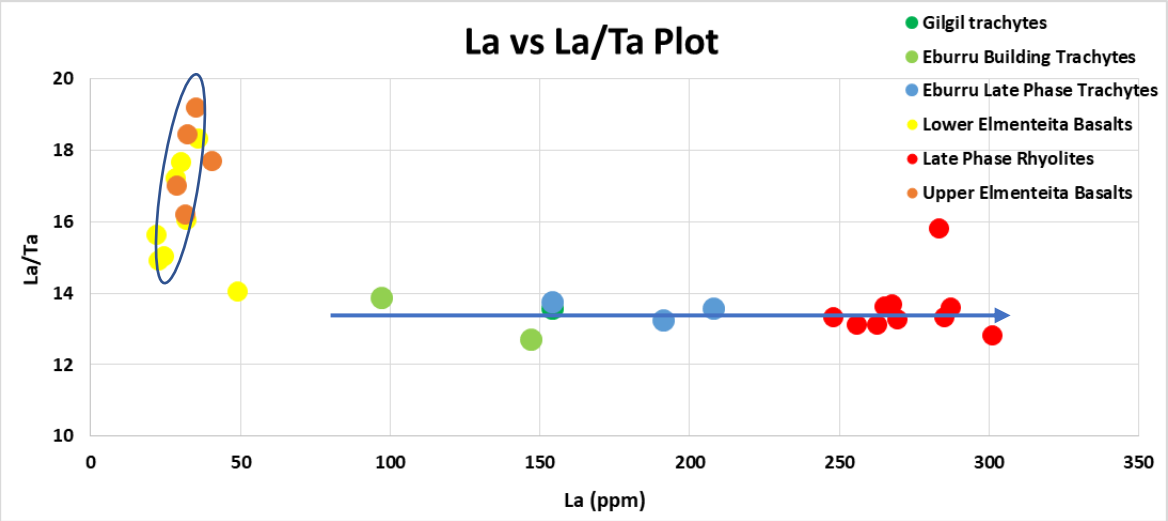

Figure 8: La vs La/Ta plot

Plots of La vs La/Tb show lower Elmenteita basalts having a ratio of 26-34, while the upper Elmenteita basalts have a ratio of 30-34 (Figure 13). Most of the trachytes have a ratio of 32-40 except one (Gilgil trachyte), which has a ratio of 50. The rhyolites have a ratio of 37-40 except for one sample (47B) that has a ratio of 47. In this plot, Ta is more incompatible than La and therefore is enriched in the liquid phase relative to La. The plot also suggests that the trachytes and rhyolites may have similar origins and evolved through fractional crystallization. More so, the Late-phase trachytes and the Eburru rhyolites. The plot also shows that the basaltic flows have a different source and may not be related among themselves via fractional crystallization.

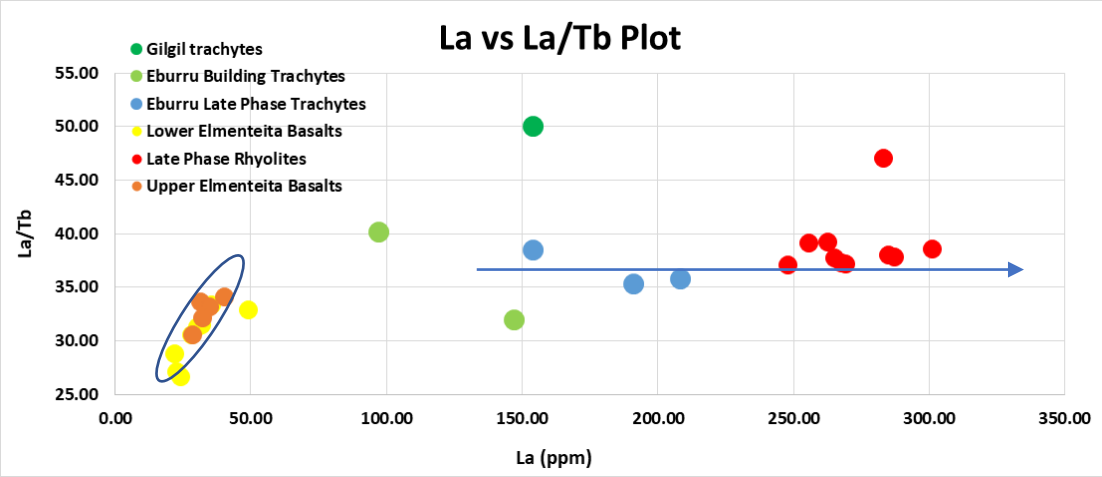

Figure 9: La vs La/Tb plot

The plot of La vs La/Hf shows Elmenteita basalts of the lower and upper series having a ratio of 7-9 while the trachytes have a ratio of 6-8 and the rhyolites have a ratio of 6-7 (Figure 14). The graph shows three populations comprising the basalts, trachytes and rhyolites with distinct La/Hf ratios. The data suggest that the three groups may all not be related.

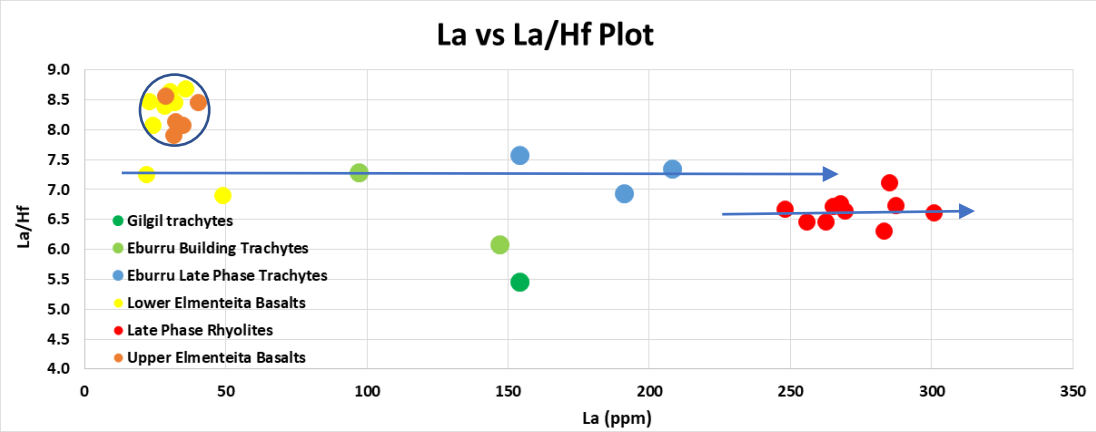

Figure 10: La vs ratio of La/Hf plot

The plot of La vs La/Zr also shows three populations with Elmenteita basalts having a ratio of 0.17-0.24 while rhyolites have a ratio of 0.15-0.17 and trachytes showing a wide scatter (Figure 15). The graph clearly indicates that the rhyolites and basalts are not cogenetic, while it may be possible that the Late-phase trachytes are related to the Late-phase Eburru rhyolites.

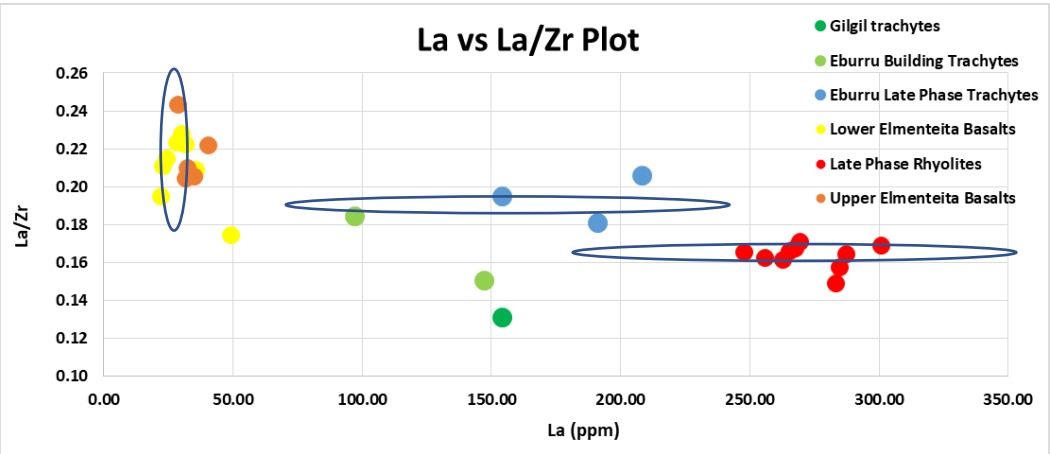

Figure 11: La vs ratio of La/Zr plot

A plot of Ta vs Ta/Tb shows Elmenteita basalts having a ratio of 1.7-2.4 while the Eburru Late-phase trachytes have a ratio of about 2.6 which is within the same range as of Late-phase rhyolites (Figure 16). The graph demonstrates the possible relationship between the Eburru Late-phase rhyolites and Late-phase trachytes.

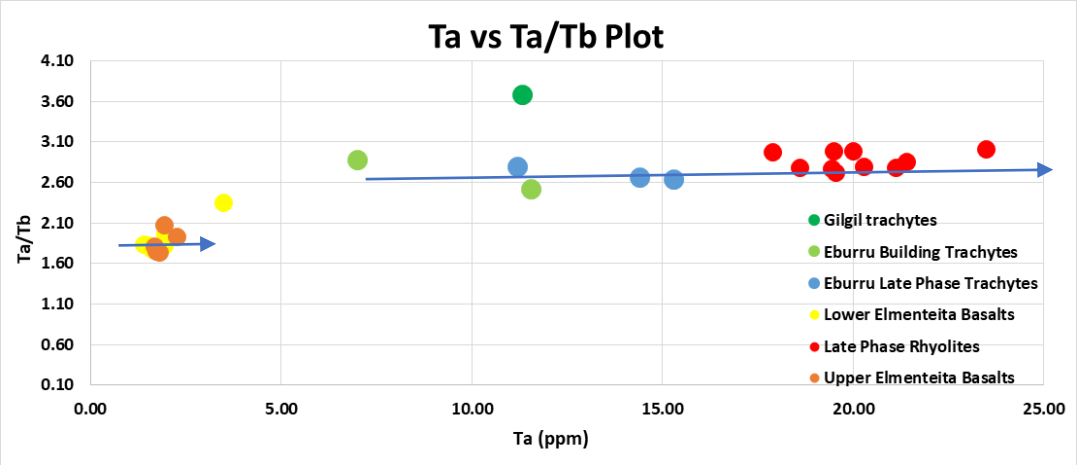

Figure 12: Ta vs ratio of Ta/Tb plot

A plot of Ta vs Ta/Ce (Figure 17) shows Elmenteita basalts of the lower series having a ratio of 0.03-0.04, while the upper Elmenteita basalts have a ratio of 0.02-0.03. The trachytes have a ratio of 0.04-0.05, while the rhyolites have a ratio of 0.03-0.05. This graph suggests that the rocks in the Otutu rift comprise four populations. However, the slight difference in the ratios could also be due to crustal contamination of the various magma batches.

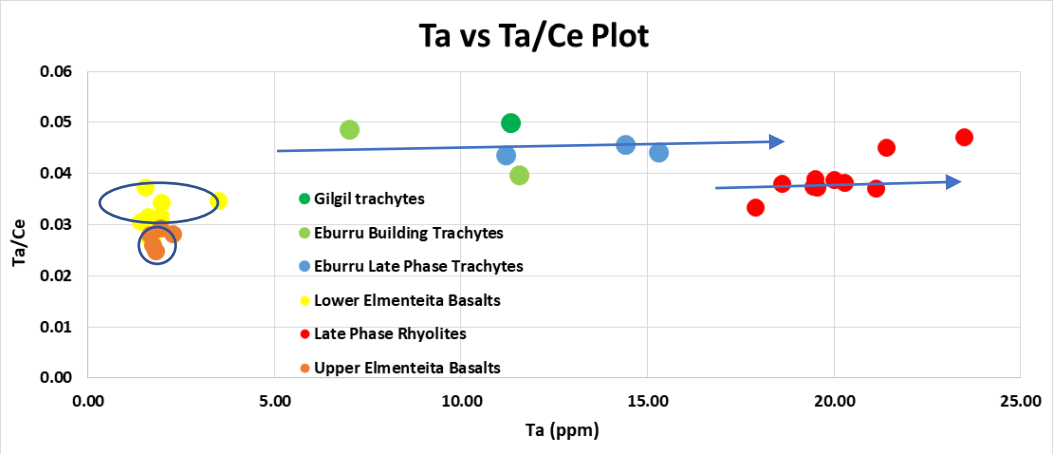

Figure 13: Ta vs ratio of Ta/Ce plot

A plot of Tb vs Tb/Hf shows Elmenteita basalts of the lower series having a ratio of 0.21-0.31 while the upper Elmenteita basalts have a ratio of 0.24-0.28 (Figure 18). The trachytes have a ratio of 0.13-0.19, while the rhyolites have a ratio of 0.11-0.20. Three distinct populations can be discerned in the graph.

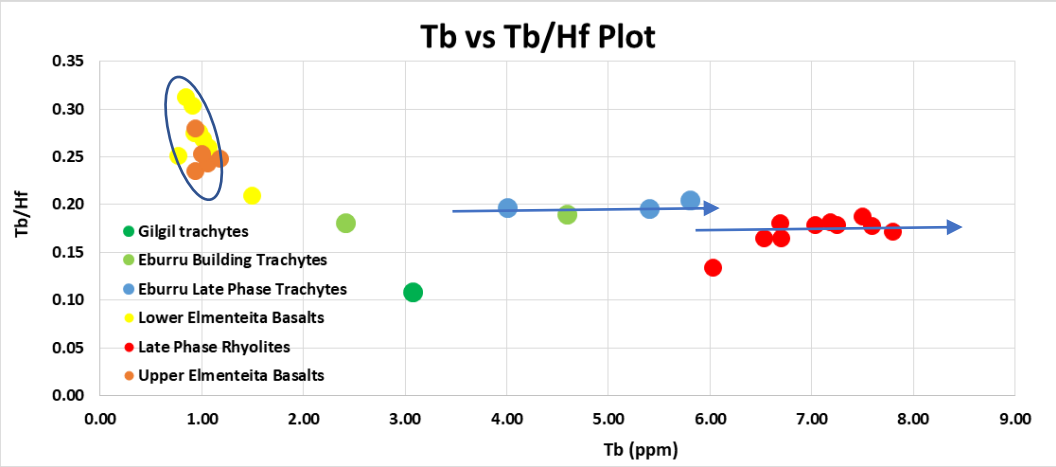

Figure 2.3.14: Tb vs ratio of Tb/Hf plot

A plot of Tb vs Tb/Ce shows that the Lower and Upper Elmenteita basalts have a Tb/Ce ratio of 0.22-0.3 (Figure 19). The Eburru Late-phase trachytes have a ratio of 0.20 while the Late-phase rhyolites have a ratio of 0.175. The ratio of Tb/Ce indicates that the

basalts groups are different, while the Late-phase trachytes and Late-phase rhyolites show different ratios but are nearly the same. The diagram clearly discriminates the basalts from the trachytes and rhyolites.

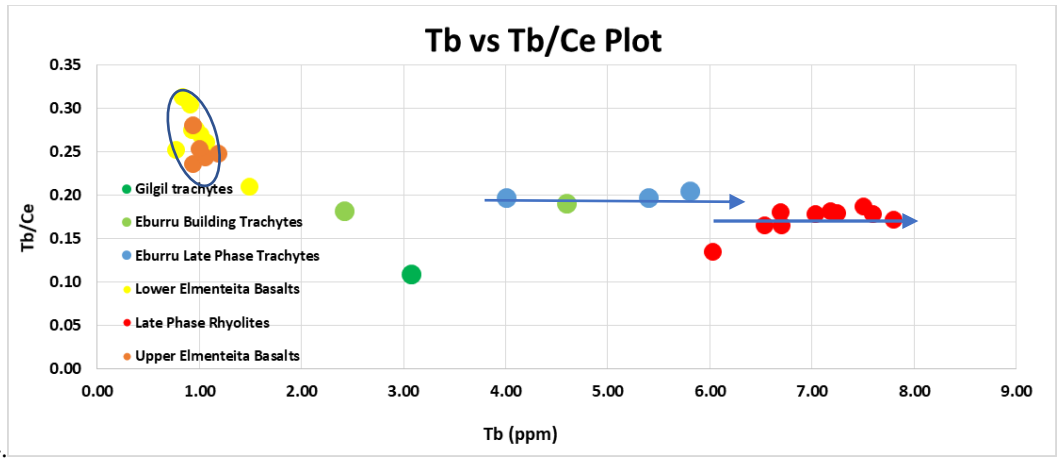

-.

Figure 15: Tb vs ratio of Tb/Ce plot

A plot of Hf vs Hf/Ce shows Elmenteita basalts of the lower series having a ratio of 0.055-0.071 while the Upper Elmenteita basalts have a ratio of 0.055-0.060 (Figure 20). The Late-phase trachytes and rhyolites have a ratio of about 0.08. The diagram suggests that the Late-phase Eburru trachytes and the Late-phase rhyolites could be related through fractional crystallization. The Elmenteita basalts are clearly distinct, and among themselves, they also seem to have different petrogenesis.

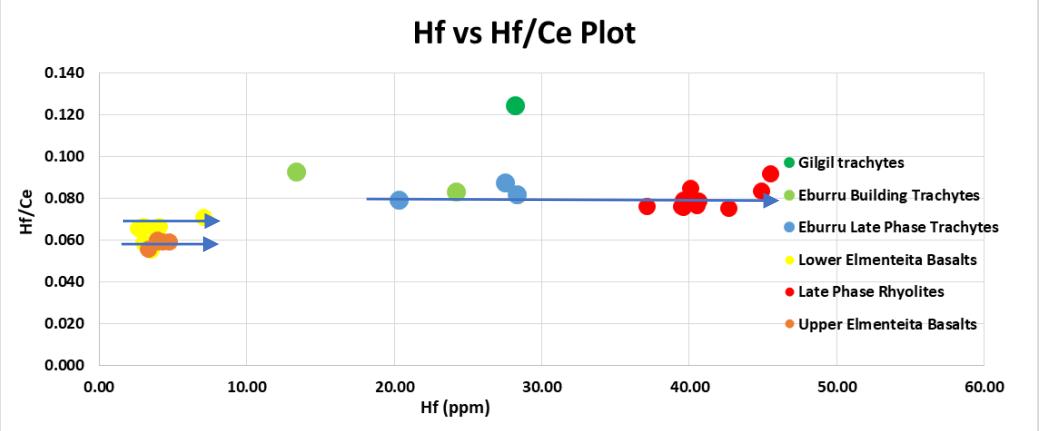

Figure 16: Hf vs ratio of Hf/Ce plot

From the plots above, the two basalts populations have different elemental ratios, and therefore, it can be concluded that the Lower and Upper Elmenteita basalts have different mantle sources. It can further be discerned from the plots that the Upper basalts may not be comagmatic among themselves as each of the sampled lava flows have different element ratios. It is also noted that the two basaltic suites have quite different elemental ratios compared to the trachytes and rhyolites. Therefore, it can be concluded that they do not share common mantle sources.

The plots also show that the Late-phase trachytes and Late-phase rhyolites have close to common elemental ratios except in few cases. The lavas also occupy space in proximity to one another. The near similar ratios suggest that the Late-phase trachytes and rhyolites are associated and share a common mantle source. Both trace and major oxides suggest that the lavas share a common transitional basalt similar to but not the same as the Elemntaita basalts and then experienced protracted fractional crystallization that involved crystal fractionation of olivine, pyroxenes, oxides, and feldspars.

(b) Rare Earth Elements (REE)

Multi elements were normalized (chondrite normalized REE) and thereafter plotted for the study area to show the evolution chemistry, and this is illustrated in Figures 21 to 27.

One can observe a regular and parallel increase in REE elements with the evolution from basalt to rhyolites.

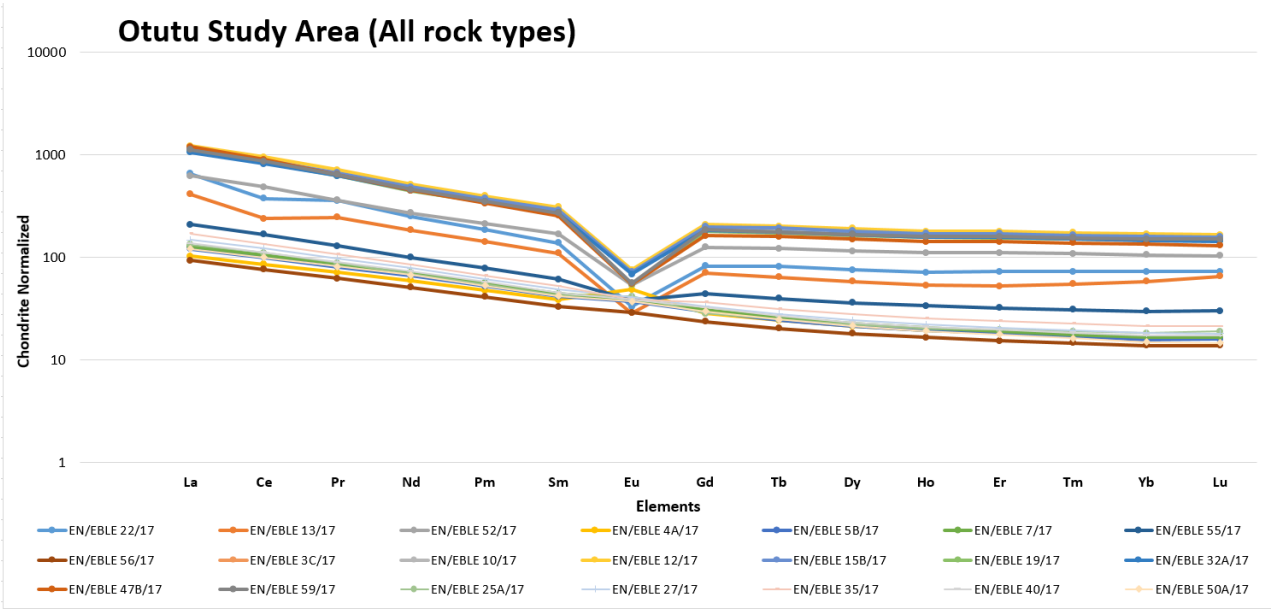

Figure 17: REE vs Chondrite normalized for all chemically analysed sampled rocks from the Otutu study area

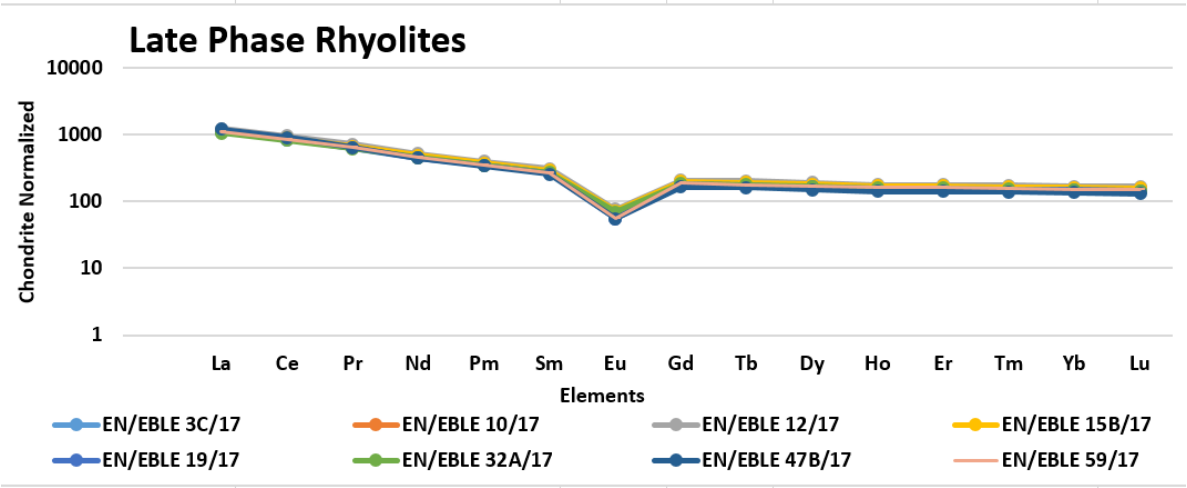

Figure 18: REE vs Chondrite normalized for the Late-phase rhyolite in the Otutu study area

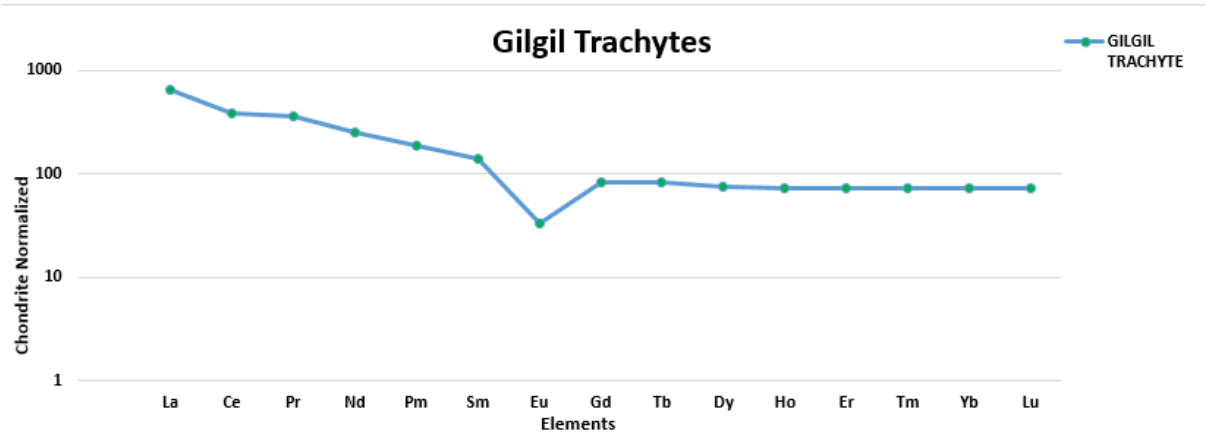

Figure 19: REE vs Chondrite normalized for the Gilgil trachyte in the Otutu study area

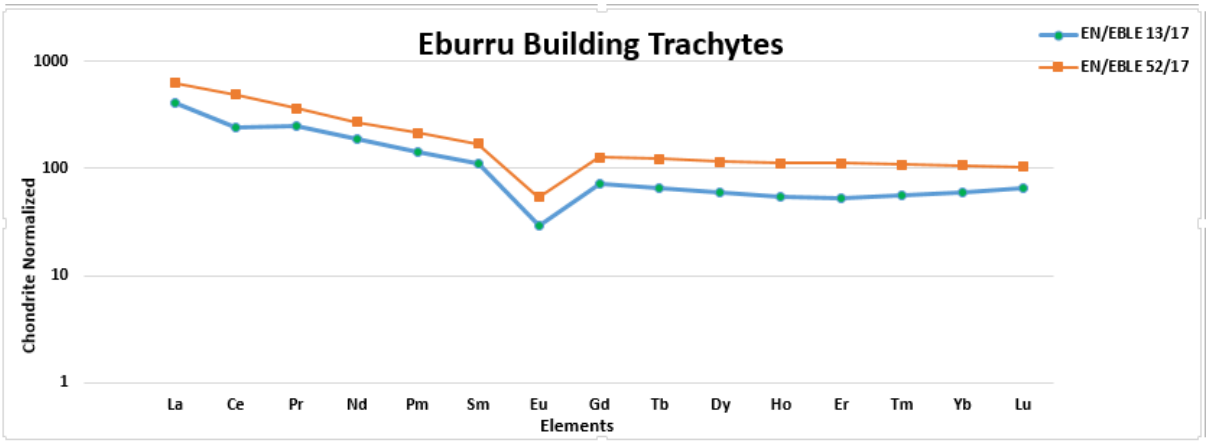

Figure 20: REE vs Chondrite normalized for the Eburru shield-building trachyte in the Otutu study area

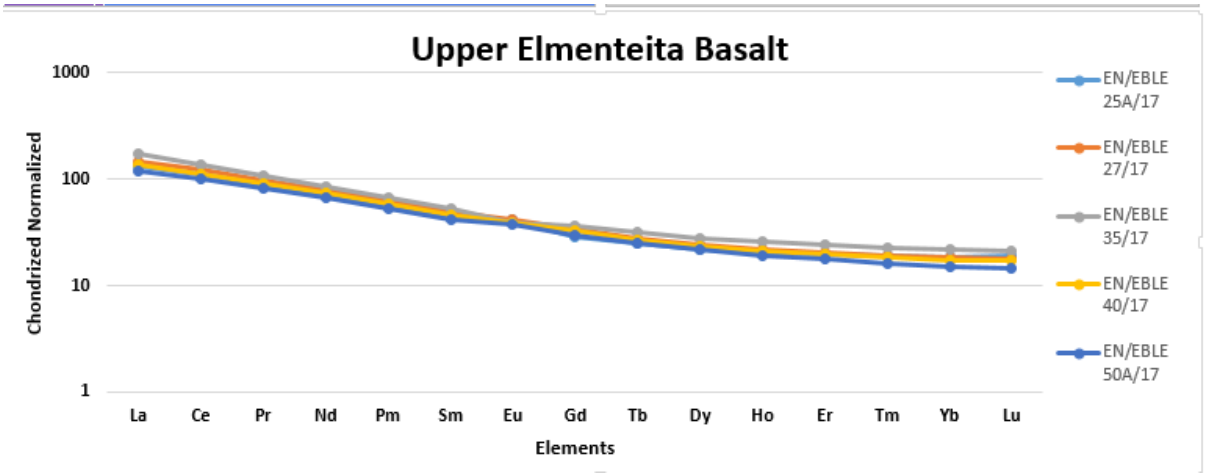

Figure 21: REE vs Chondrite normalized for the Upper Elmenteita basalt in the Otutu study area

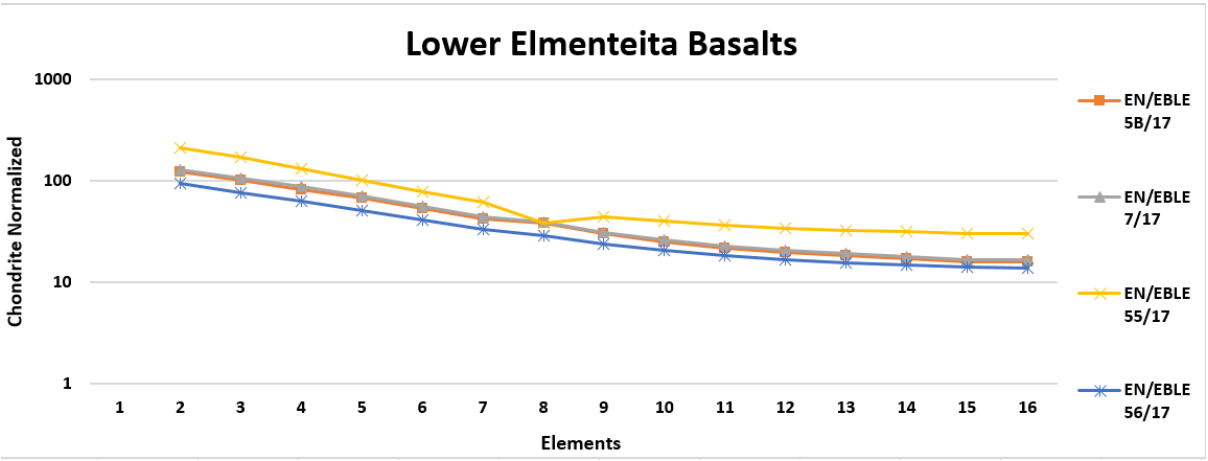

Figure 22: REE vs Chondrite normalized for the Lower Elmenteita basalt in the Otutu study area

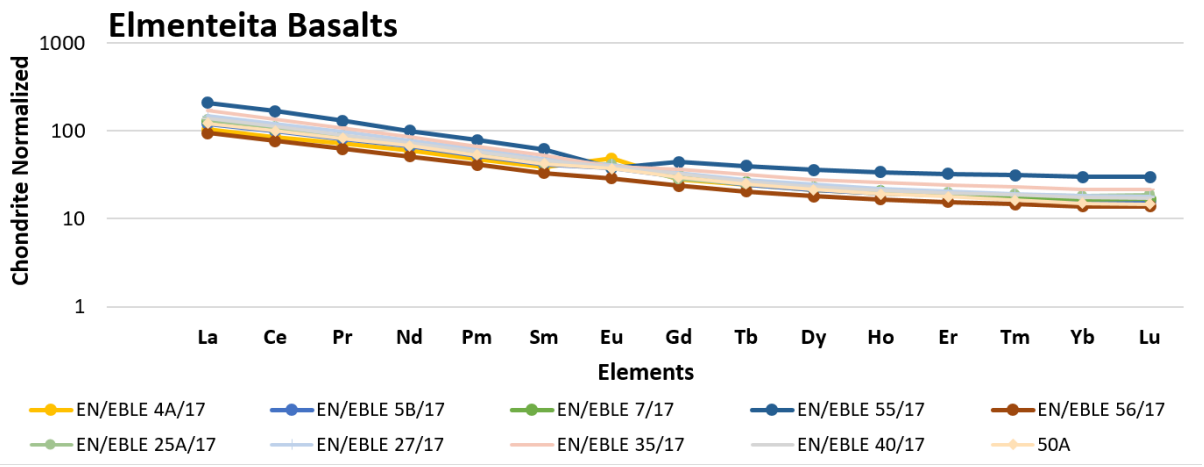

Figure 23: REE vs Chondrite normalized for the Elmenteita basalt (Lower and Upper basalts) in the Otutu study area

From the above diagrams, it is noted that there is a strong negative europium anomaly in trachyte and rhyolites due to the fractionation of feldspars. Barberi et al., (1975) described the negative Eu anomaly as resulting from the fractionation of alkali-feldspars since the element is incorporated in the lattice structure of the minerals.

3. CONCLUSION

The Otutu study area is characterized by several volcano-structural features that include fissures, recent basaltic lava flows and shield structures. Important heat release along the rift axis is also noted in the area. Steam vents are aligned along open fissures and faults synchronous and post-dating the volcanic events. Several hydrothermal zones are also noted in the area. Though there are other rock types that fall out of the fractionation line (the Gilgil Trachyte, the basalts sampled outside the rift axis and the Eburru rhyolites) but most rock types sampled within the rift axis of the study area still display a nice fractionation line. This clearly indicates the presence of a shallow steam-dominated reservoir underlying the study area. This reservoir is possibly heated by the underlying magma chamber beneath it. The results also show that after the widespread trachyte emission that pre-dated the formation of the present rift, a variety of volcanic products were emitted. These happened during each of the successive steps of the rift segment development. The emission ranged from alkali-olivine basalts to pantellerites, with a few intermediate types. This means that, geothermally, the Otutu rift is not only fed by the fissural basalts originating from a deep-seated source but also from a shallow, elongated magma chamber that is along the rift axis.

Petrological investigations in this study allowed for the identification of the bimodal nature of the rocks in the area. The area has a large variety of both basic and acidic rocks. This variety of lava rocks ranged from alkali olivine basalts to mugearites, trachytes and pantelleritic obsidians, with a relative abundance of the later. Petrological analysis of the rocks and their interpretation shows that this evolution can simply be explained by the process of crystal fractionation occurring in the crust a few kilometres deep. It, therefore, appears that this linear volcano-tectonic context dominated by fissure eruptions along the rift axis allowed for this magma development. This could have occurred during the last few hundred thousand years. Successive magma chambers seem to be elongated along the same axis with successive rejuvenations through basaltic magma injection from the relatively shallow underlying anomalous mantle.

Geochemical analysis carried on the selected fresh aphyric rock samples provided a complete view of the various kind of liquids emitted during the last million years along this active segment of the rift. The results showed that very dynamic magmatism had taken place that resulted in differentiation. This is evidenced by the different rock suites noted: basalts, trachytes and rhyolites. By use of trace elements, it is concluded that the magma sources for the various rock suites are at least three. This is due to the noted different elemental ratios noted in the plotted graphs. Incompatible elements ratios are less affected by FC than other element abundances. The ratios are usually similar in geochemical behavior, and rocks that are related by FC have a common/constant ratio. Therefore, the ratio of two incompatible elements in a magma will be more or less the same as that in the magma source.

The geological data collected in the field, the rock sample analysis, and the interpretation of the results in terms of geothermal implications have been included in a global geoscientific approach, thus allowing for a new conceptual model of the geothermal system in the rift segment to be proposed. As a result of the crystal fractionation and differentiation, this study alludes to presence of magma chambers below the study area. These results are thought to be of interest for the future development of the area, as well as – more generally – the search for new geothermal resources along the East African Rift System away from the central volcanic units along other active rifts segments, which represent much wider areas than the ones presently being targeted. Therefore, the possible heat source (s) in this type of environment should be investigated further and even exploited even if they differ in terms of size and shape with the central volcanoes.

4. RECOMMENDATIONS

The field work (rock-suites mapping), samples collection and analysis for major and trace element geochemistry provided only a limited insight into the petrogenesis of the Otutu rift. There is a need to undertake further studies in this area. The following studies are recommended: geochronological studies, a further detailed mineralogical study of a few key phases determining the major shifts in the fractionation process (e.g. how the amphibole pass from nepheline basalts to quartz trachytes and plagioclase pass from meta-aluminous to peralkaline liquids), close-knit geophysical surveys (preferably MT and magnetic surveys) to clearly map out the

anomalies (thin, elongated heat sources), radiogenic isotope analysis, geochronological studies to evaluate not only the actual ages of the various rock series but also to quantify the periodicity of the magma injection and differentiation. This would go a long way in better understanding of this spreading axis in order to properly model the vertical dimensions of the rift segment and quantitatively define the whole geothermal conceptual model of this rift segment through the tectono-magmatic history.

REFERENCES

Bach, W., Hegner, E., Erzinger, J. and Satar, M. (1994). Chemical and Isotopic Variations Along The Superfast Spreading East Pacific Rise From 6 To 30º S, Contrib. Mineral. Petrol., V.116, pp.365-380.

Barberi F., and Varet J. (1975) - Recent volcanic units of Afar and their structural significance. In: Pilger A., and Rösler A. (edit.), Afar Depression of Ethiopia, Stuttgart (Schweizerbart), p. 174-178.

Clarke, M.C.G., Woodhall, D.G., Allen, D.J., Darling, W.G. (1990). Geological, Volcanological, and Hydrogeological Controls on the Occurrence of Geothermal Activity in the Area Surrounding Lake Naivasha, Kenya. Ministry of Energy, Kenya and British Geological Survey, Nairobi. pp138.

Lagat J. (2004). Geology, Hydrothermal Alteration and Fluid Inclusion Studies Of Olkaria Domes Geothermal Field, Kenya. MSc Thesis, University of Iceland.

McCall G. J. H. (1957). Geology and Ground Water Conditions in the Nakuru Area. Ministry of Environment and Natural Resources Mines and Geological Department Geology and Ground Water Conditions in the Nakuru Area. Technical Report No. 3, pp22-27.

Perfit, M.R., Fornari, D.J., Ridlay, W.I., Kirk, P.D., Casey, J., Kastens, K.A., Reynolds, J.R., Edwards, M., Desonie, D., Shuster, R. And Paradis, S. (1996). Recent Volcanism in the Siqueiros Transform Fault: Picritic Basalts and Implications for Morb Magma Genesis. Earth Planet. Sci. Lett., V.141, pp91-108.

Perfit, M.R., Fornari, D.J., Smith, M.C., Bender, J.F., Langmuir, C.H. And Haymon, R.M. (1994) Small-Scale Spatial And Temporal Variations In Mid-Ocean Ridge Crest Magmatic Processes, Geology., V.22, pp. 375-379.

Perfit, M.R. (2001) Mid-Ocean Ridge Geochemistry and Petrology. Academic Press, University Of Florida, P.11.

Reynolds, J.R., Langmuir, C.H., Bender, J.F., Kastens, K.A. And Ryan, W.B.F. (1992) Spatial And Temporal Variability In The Geochemistry Of Basalts From The East Pacific Rise. Nature, V.359, Pp.493-499

Sims, K.W.W., Goldstein, S.J., Blicher-Toft, J., Perfit, M.R., Kelemen, P., Fornari, D.J., Murrell, M.T., Hart, S.R., Depaolo, D.J., Layne, G., Ball, L., Jull, M.V. And Bender, J. (2002). Chemical And Isotopic Constraints On The Generation And Transportation Of Magma Beneath The East Pacific Rise. Geochim. Cosmochim. Acta, V.66(19), pp3481-3504.

Varet, J. (2017). Unpublished Report on Badlands (West from Gilgil): Structural Geology, Volcanology and Igneous Rocks Petrology. DeKUT/Géo2D for KenGen.

Wendt, J.I., Regelous, M., Niu, Y., Hekinian, R. And Collerson, K.D. (1999). Geochemistry Of The Lavas From The Garret Transform Fault: Insights From The Mantle Heterogeneity Beneath The Eastern Pacific. Earth Planet. Sci. Lett., V.173, pp.271-284.